

Non-Equilibrium Gating in Cardiac Na⁺ Channels An Original Mechanism of Arrhythmia

Colleen E. Clancy, PhD; Michihiro Tateyama, PhD; Huajun Liu, MD;
Xander H.T. Wehrens, MD, PhD; Robert S. Kass, PhD



Background—Many long-QT syndrome (LQTS) mutations in the cardiac Na⁺ channel result in a gain of function due to a fraction of channels that fail to inactivate (burst), leading to sustained current (I_{sus}) during depolarization. However, some Na⁺ channel mutations that are causally linked to cardiac arrhythmia do not result in an obvious gain of function as measured using standard patch-clamp techniques. An example presented here, the SCN5A LQTS mutant I1768V, does not act to increase I_{sus} (<0.1% of peak) compared with wild-type (WT) channels. In fact, it is difficult to reconcile the seemingly innocuous kinetic alterations in I1768V as measured during standard protocols under steady-state conditions with the disease phenotype.

Methods and Results—We developed new experimental approaches based on theoretical analyses to investigate Na⁺ channel gating under non-equilibrium conditions, which more closely approximate physiological changes in membrane potential that occur during the course of a cardiac action potential. We used this new approach to investigate channel-gating transitions that occur subsequent to channel activation.

Conclusions—Our data suggest an original mechanism for development of LQT-3 arrhythmias. This work demonstrates that a combination of computational and experimental analysis of mutations provides a framework to understand complex mechanisms underlying a range of disorders, from molecular defect to cellular and systems function. (*Circulation*. 2003;107:2233-2237.)

Key Words: arrhythmia ■ remodeling ■ sodium ■ long-QT syndrome

Ion channels are a diverse group of pore-forming transmembrane proteins that selectively conduct ions and play physiological roles in most cell types, including neurons, skeletal muscle, smooth muscle, and cardiac muscle. Inherited mutations in genes encoding ion channels have been associated with such a large number of human diseases, including epilepsy, febrile seizures, Dent's disease, and cardiac arrhythmias, that the disorders are called "channelopathies."¹⁻⁷ Expression of ion channels in heterologous systems allows for investigation of inherited ion channel defects at the single protein and cellular level to directly identify the disease-associated alterations in ion channel function. Disease-linked mutations provide an opportunity to understand the mechanistic basis of human disease, from altered molecular function to the clinical syndrome. This approach has led to novel insight into roles of key ion channels in human physiology and pathophysiology.

Perhaps one of the most unexpected and interesting revelations is the link between mutations in SCN5A, the gene coding for the α -subunit of the cardiac Na⁺ channel, and variant 3 of the long-QT syndrome (LQT-3), a disease in

which ventricular repolarization is prolonged.⁸ Investigation of the disease-associated mutant channels revealed defects in channel inactivation such that during the prolonged plateau phase of the cardiac ventricular action potential, a small number of channels reopen and conduct Na⁺ ions instead of entering an absorbing non-conducting inactivated state, creating sustained Na⁺ current (I_{sus}).⁹ This mutation-altered channel function was demonstrated in computational models and in genetically altered mice to account for the disease phenotype.^{10,11} Recently, mutations in SCN1A, the gene coding for the human neuronal Na⁺ channel α -subunit, that are associated with epilepsy have been reported to cause similar defects in channel inactivation gating and promotion of I_{sus} .⁵ As of yet, the cellular consequences of such epilepsy mutations remain elusive. Thus, mechanistic insights gained from investigation of cardiac defects are likely to have widespread implications.

However, not all LQT-3 mutations in SCN5A cause this type of altered channel behavior, and understanding how these other mutations cause the disease phenotype, manifested as prolongation of the ECG QT interval, has not been

Received February 24, 2003; revision received March 13, 2003; accepted March 13, 2003.

From the Department of Pharmacology, Columbia University College of Physicians and Surgeons, New York, NY.

The online-only Data Supplement is available at <http://www.circulationaha.org>.

This article originally appeared Online on April 14, 2003 (*Circulation*. 2003;107:r70-r74).

Correspondence to Robert S. Kass, PhD, Department of Pharmacology, Columbia University College of Physicians and Surgeons, 630 W 168th St, New York, NY 10032. E-mail rsk20@columbia.edu

© 2003 American Heart Association, Inc.

Circulation is available at <http://www.circulationaha.org>

DOI: 10.1161/01.CIR.0000069273.51375.BD

obvious based on the analysis of mutant channel biophysical properties. Examples of mutations that do not result in gain of function include D1790G, E1295K, and I1768V.^{12–14} These defect types led us to ask, how might mutations that have subtle effects on channel kinetics underlie severe patient phenotypes? Can we investigate Na⁺ channel gating differently to reveal arrhythmia cellular mechanisms and altered channel function that might be relevant to other diseases?

The approach we have taken was to use computer modeling to first analyze theoretical and subtle changes in channel gating that might underlie the disease phenotype, but which may have been overlooked in previous experimental investigations. We utilized a theoretical cardiac Na⁺ channel model^{10,15} to guide our experimental approach to investigate genetic defects.^{16–18} The model suggested that mutation-altered gating transitions subsequent to channel activation, driven by changes in membrane potential during repolarization, might determine action potential duration. Because recovery from open-state inactivation is time- and voltage-dependent, standard voltage clamp protocols may fail to reveal mutation-induced changes in kinetics that exist under conditions in which voltage changes.

We chose to focus on the I1768V LQT3 mutation in the cardiac Na⁺ channel because a previous study that investigated alterations in steady state channel gating revealed that the mutation sped recovery from inactivation.¹³ In that study, a long slow (steady-state) positive ramp protocol also revealed subtle changes in window current, which were suggested as a potential arrhythmia mechanism. In the present study, our computational analysis led us to believe that faster recovery from open state inactivation in I1768V may be the major factor in determining disease phenotype.

We provide experimental evidence in support of this hypothesis and propose that mutation-induced gain of function in cardiac sodium current (I_{Na}) can exist in at least 3 distinct forms. The most common is due to transient inactivation failure, termed bursting, which underlies sustained Na⁺ channel activity over the plateau voltage range.^{9,19} A second is due to steady-state channel reopening called window current,²⁰ because reopening occurs over voltage ranges for which steady-state inactivation and activation overlap. Here we demonstrate a third original mechanism that occurs under non-equilibrium conditions whereby channel reopening results from faster recovery from inactivation at membrane potentials that facilitate the activation transition. We find that mutation induced faster recovery from inactivation results in channels that reopen during repolarization and that the resulting current amplitude rivals that of bursting channels. Using the Luo-Rudy virtual transgenic cell,²¹ we demonstrate that late current due to channels reopening causes severe prolongation of the AP plateau and arrhythmic triggers.

Methods

Expression of Recombinant Na⁺ Channels

Na⁺ channels were expressed in human embryonic kidney 293 cells at 22°C as described previously.¹⁴ CD8-positive cells identified using Dynabeads (Dyna, M-450) were patch clamped 48 hours after transfection.

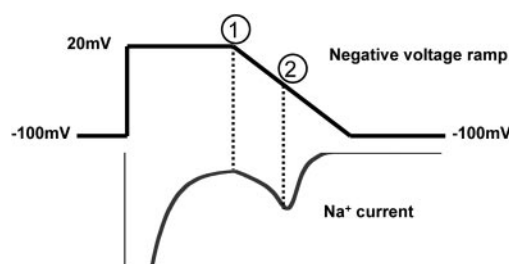


Diagram. A schematic of the voltage protocol. Persistent late current I_{sus} was measured after 100 ms depolarization to +20 mV, indicated by ① in the diagram. Ramp currents (I_{ramp}) were measured as the peak inward current during the negative ramp (indicated as ②).

Electrophysiology

Membrane currents were measured using whole cell patch-clamp procedures, with Axopatch 200B amplifiers (Axon Instruments). Capacity current and series resistance compensation were carried out using analog techniques according to the amplifier manufacture (Axon Instruments). All measurements were obtained at room temperature (22°C). Macroscopic whole cell Na⁺ current was recorded using the following solutions (mmol/L). The internal solution contained aspartic acid 50, CsCl 60, Na₂-ATP 5, EGTA 11, HEPES 10, CaCl₂ 1, and MgCl₂ 1, with pH 7.4 adjusted with CsOH. The external solution contained NaCl 130, CaCl₂ 2, CsCl 5, MgCl₂ 1.2, HEPES 10, and glucose 5, with pH 7.4 adjusted with CsOH. Using WEBMAXCLITE v1.15,²² at 22°C at pH 7.4 and ionic strength = 0.16N, we computed the free Ca²⁺ and Mg⁺ as 6.888e-9 mol/L and 0.000245 mol/L, respectively. The voltage protocols are described in the text. Negative ramp currents were measured as tetrodotoxin (TTX)-sensitive current by applying TTX at high concentrations (30 μmol/L) to block expressed Na⁺ channel currents and reveal background currents, which were then subtracted digitally. A schematic of the voltage protocol is shown in the Diagram. Persistent late current I_{sus} was measured after 100 ms depolarization to +20 mV, indicated by ① in the diagram. Ramp current (I_{ramp}) was measured as the peak inward current during the negative ramp (indicated as ② in the Diagram). Holding potentials were -100 mV. Analysis was performed in Excel (Microsoft) and Origin 6.1 (Microcal Software). Data are represented as mean ± SEM. Statistical significance was determined using unpaired Student's *t* test; $P < 0.05$ was considered statistically significant.

Computational Methods

All computational methods have been described in previous publications.^{10,15} Action potentials were computed by incorporating this model of I_{Na} into a previously described cellular model.¹⁵

Model Framework

Mutant channels differ from WT channels in one distinct way, as evidenced by experimental recordings. Mutant channels have altered rates of recovery from channel inactivation due to faster rates of recovery from channel inactivation (Data Supplement). The faster recovery from inactivation is simulated in mutant I1768V channels by doubling the rates of recovery from inactivation (UIM2 → UIM1, UIM1 → UIF, UIC3 → UC3, UIC2 → UC2, UIF → UC1) transitions.

The Markov model of I_{Na} is shown in the Data Supplement. The model contains 2 possible modes of gating, a “background mode” and a “burst mode.” The background mode includes the upper 9 states, which consist of 3 closed states (UC3, UC2, UC1), a conducting open state (UO), a fast inactivation state (UIF), and 2 intermediate inactivation states (UIM1 and UIM2) that are required to reproduce the complex fast and slow recovery features of inactivation. Channels enter the IM2 state via slow transitions. Channel closed-state inactivation is achieved via the inclusion of 2 closed inactivation states (UIC2 and UIC3). The lower four states

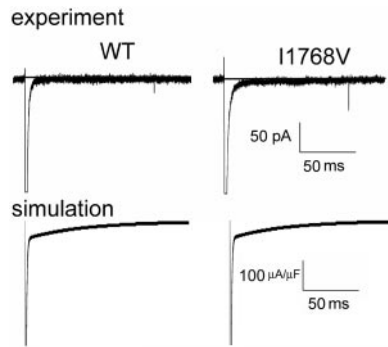


Figure 1. The I1768V mutation (right) has little effect on whole cell currents compared with wild-type (left) in experiments (top, line indicates zero current level) and simulations (bottom).

(prefixed with L, denoting “lower”) correspond to a burst mode of gating that corresponds to channels that lack inactivation. This population is unchanged by the I1769V mutation and is negligible but included for accuracy in both WT and I1768V mutant channels (<0.07% of peak current after 100 ms depolarization to +20 mV). Transition rates between upper and lower states represent a probability of transition between the 2 modes of gating. Microscopic reversibility was ensured by fixing the products of the forward and reverse transition rates in closed loops of the model.

All the simulations were encoded in C/C++. Simulations were implemented (double precision) on an Apple Macintosh 500 mHz G4 Powerbook (Motorola) running OS X. A time step of 0.005 ms was used.²³ Computer code used for computations in this paper is available on request by e-mailing cc2114@columbia.edu.

Results

The effects of the I1768V mutation on steady-state currents were previously reproduced by incorporating a 2-fold increase in the rate of recovery from channel inactivation in a computer model of cardiac Na⁺ channel current (I_{Na}) (Data Supplement).¹⁵ Faster recovery from inactivation had no effect on current density, sustained current (channel bursting), activation (not shown), or the voltage-dependence and time course of currents activated during depolarization (Figure 1, lower), consistent with experimental data (Figure 1, upper).

We next investigated non-equilibrium gating of WT and I1768V channels using a theoretical and then an experimental approach. We computed currents (I_{ramp}) using a negative ramp protocol. In the computation, cells first were depolarized (+20 mV for 100 ms from holding potential [V_h]=−100 mV) to promote open state inactivation. As noted previously, at this voltage, after opening, channels enter an absorbing inactivated state and there is very little sustained current (measured after 100 ms at +20 mV, indicated by arrows in Figure 2A). Gradual repolarization was then applied over 100 ms until V_h =−100 mV, allowing for recovery from inactivation. We first used the model to investigate the consequences of an increased rate of recovery from inactivation on current during a repolarizing ramp (I_{ramp}) and 100 ms depolarization to −20 mV (I_{sus}). In the simulation, a 2-fold increase in the channel recovery rate results in nearly a doubling of the peak current (I_{ramp}) elicited by the negative ramp for the I1768V mutation (−1.23A/F, 0.2% of peak current [−581.6A/F]) compared with WT (−0.738A/F, 0.1% of peak current [−580.0A/F]) (Figure 2A), but no difference

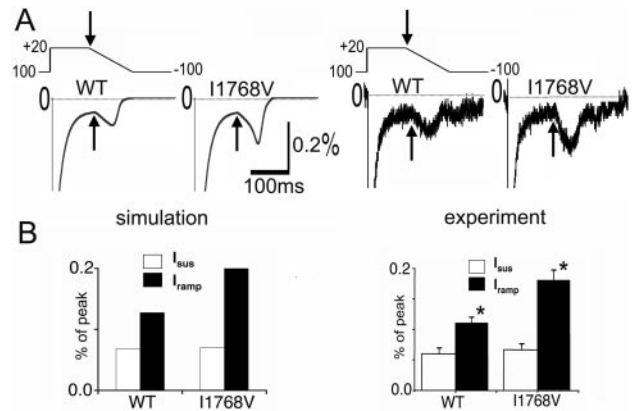


Figure 2. A, Non-equilibrium gating. Simulated (left) and experimental (right) macroscopic currents during the negative ramp protocol (see text). B, Summary of I_{sus} (plotted as % peak current, measured at time indicated by arrows in A) after 100 ms depolarization to +20 mV (I_{sus} , reflects bursting channels) and peak current during the ramp repolarization (plotted as % peak current) (I_{ramp} , reflects channel reopenings). There is no significant difference between I_{sus} WT and I_{sus} I1768V. For I_{ramp} , there is a significant difference in maximum ramp current between WT and I1768V channels. Number of experiments: $n=6$, WT; $n=10$, IV. * $P=0.02$.

between I_{sus} in WT (−0.39A/F, 0.07%) or I1768V (−0.40A/F, 0.07%) simulated cells (Figure 2A) was noted. The arrows in Figure 2A indicate the end of the 100 ms depolarization, when I_{sus} was measured. Summarized data are shown as percentages of peak current in Figure 2B, left.

Consistent with the computations, we found that I1768V mutants expressed in human embryonic kidney 293 cells exhibit larger transient inward current (−0.33A/F, 0.18% of peak current [−202.1A/F]) during repolarization than WT channels (−0.31A/F, 0.12% of peak current [−259.1A/F]) (Figure 2A) with no change in bursting, because late current measured after 100 ms depolarization to −20 mV (arrow in Figure 2A) is identical in WT (−0.14A/F, 0.05%) and I1768V (−0.13A/F, 0.06%) channels. Again, the arrows indicate the end of the 100 ms depolarization when I_{sus} was measured. Importantly, the larger current is not window current, as the voltage of peak I_{ramp} occurs outside the overlap of activation and inactivation (WT peak I_{ramp} occurs at −24.17 mV \pm 3.26, IV peak I_{ramp} occurs at −18.89 mV \pm 1.49). Summary data for experimentally determined I_{sus} and I_{ramp} are presented in Figure 2B, right panel. The experimental result is nearly identical to the theoretical simulation; I_{sus} is the same for WT and IV channels (0.05 \pm 0.01%, $n=6$; and 0.07 \pm 0.07%, $n=6$, not significant, respectively), whereas I_{ramp} is significantly increased (0.12 \pm 0.006%, $n=6$; and 0.17 \pm 0.02%, $n=10$, $P=0.02$, respectively).

It should be noted that the larger I_{ramp} observed in I1768V cells is not attributable to an increase in driving force because the small fraction of current that remains at the end of the 100 ms depolarization (I_{sus}) is present in both the WT- and mutant channel-containing cells. It is also not due to longer openings in mutant channels, as the time course of the macroscopic current decay was not affected by the mutation, and previous measurements of single channels reveal identical gating.¹³

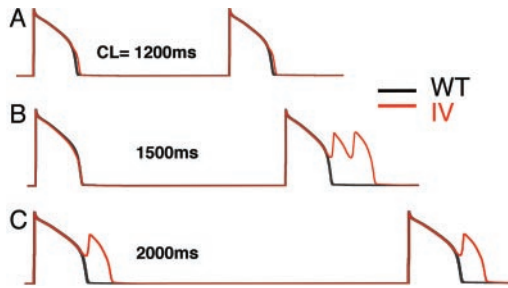


Figure 3. The I1768V mutation disrupts cellular repolarization in a rate-dependent manner. Faster recovery from inactivation resulting from the I1768V mutation results in channel reopenings during repolarization of the AP (19th and 20th paced APs), which prolongs the APD at a pacing rate of 1200 ms (A) and leads to arrhythmogenic early afterdepolarizations as the rate is slowed (B, 1500 ms; C, 2000 ms).

Is this single change in kinetics sufficient to disrupt cellular repolarization? We tested I1768V mutant channels in the Luo-Rudy model of the cardiac action potential.²¹ Effects of the I1768V (red line) mutation on cellular repolarization compared with WT (black line) at 3 pacing rates are shown in Figure 3 (A: 1200 ms, B: 1500 ms, and C: 2000 ms). The AP simulations reveal that the I1768V mutation disrupts cellular repolarization in a rate-dependent manner as described previously in the clinical phenotype.¹³ As the pacing rate is progressively slowed (Figure 3B and 3C), the I1768V mutation results in formation of arrhythmogenic early afterdepolarizations (EADs).

The mechanism of I1768V disruption of cellular repolarization is shown in Figure 4. The 19th and 20th WT (left) and I1768V (right) APs after pacing at CL=2000 ms are shown with corresponding I_{Na} at high gain. Clearly, the I1768V mutation results in a much larger inward current (arrows) compared with WT, because of faster recovery of Na^+ channels from inactivation and subsequent channel reopening. The reopenings result in a relatively large I_{Na} during the normally delicately controlled AP plateau. Indeed, the current amplitude is at least as large as that observed for the Δ KPQ mutation, known to result in severe patient phenotypes.²⁴ Moreover, the repolarization rate during the AP seems to exacerbate the channel reopenings, thereby resulting in stable development of EADs.

Discussion

Here we have used a novel approach to elucidate the link between an inherited ion channel mutation and its disease

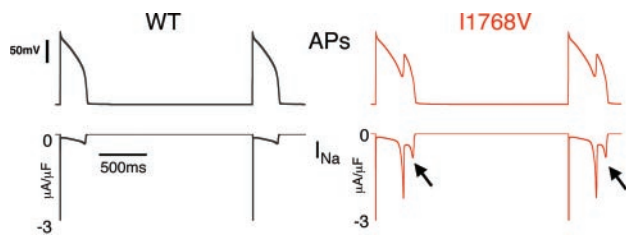


Figure 4. Mechanism of abnormal repolarization. The 19th and 20th paced (rate=2000 ms) WT (left) and I1768V (right) action potentials are shown with corresponding I_{Na} at high gain shown beneath.

phenotype. By using a computational analysis of ion channel activity, we developed targeted experiments to dissect subtle changes in channel gating that, within the framework of the computational model, were capable of causing the disease phenotype. A great advantage of analyzing the relationship between inherited defects in cardiac ion channels and the clinical disorders they cause is the fact that the electrical characteristics of the disease phenotype can be measured directly (via the ECG) and compared with the expected changes in cellular function caused by the experimentally determined alteration in channel function. Another advantage, which we demonstrate in the current study, is the utility of computational models of both cellular and ion channel electrophysiology that have been developed for cardiac cells.

In the present study, we demonstrate a third and novel mechanism by which mutations in the cardiac Na^+ channel may lead to a gain of channel function that leads to Na^+ current during the action potential plateau. The most common gain of function defect is due to transient failure of channel inactivation, a mode of gating termed bursting, which underlies sustained Na^+ channel activity over the plateau voltage range.^{9,19} A second mechanism results from steady-state channel reopening, called window current,²⁰ because reopening occurs over voltage ranges for which steady-state inactivation and activation overlap. Here, we demonstrate a third original mechanism that occurs under non-equilibrium conditions whereby channel reopening results from faster recovery from inactivation at membrane potentials that facilitate the activation transition. This third type of gain of function can be distinguished from window current by considering the voltage (-20 mV) at which the reopening occurs, which is outside of the region of overlap of the activation and inactivation curves. It should be noted that the population of channels that recover at plateau membrane potentials represents a tiny fraction of the channel population that recover more rapidly because of the channel mutation. Although recovery at plateau potentials is generally unfavorable, the mutation increases the propensity of channels to reopen under non-equilibrium conditions, ie, during changing voltage, that are not obvious during steady-state voltage protocols. We find that mutation induced faster recovery from inactivation results in channels that reopen during repolarization and that the resulting current amplitude rivals that of bursting channels. Using a virtual transgenic cell,²¹ we demonstrate that late current due to channels reopening causes severe prolongation of the AP plateau and arrhythmic triggers.

It is notable that the time-course of late I_{Na} is different during the action potential (Figure 4) compared with that observed during the negative ramp (Figure 2A). There are several things that make the current morphology different. First, the negative ramp protocol begins with a 100 ms depolarization to 20 mV, which was chosen deliberately to observe channel transitions that occur subsequent to channel open-state inactivation during the plateau phase of the action potential. The long depolarization to force channel inactivation results in a pseudo steady-state open channel inactivation, which allows for the unencumbered study of channel transitions out of these states.

In the case of the action potential, the membrane potential is constantly changing, thereby making it difficult to determine exactly which transitions are occurring at any given time. Indeed, it appears that the rate of change of the membrane potential during the action potential promotes channel reopening even more than that observed during the negative ramp. This occurs because the action potential upstroke is followed by immediate repolarization. Hence, fewer channels enter intermediate inactivation states, increasing the likelihood of reopening. In Figure 4, the I1768V Na⁺ current exhibits 2 late Na⁺ peaks during AP repolarization. The first peak (2.2A/F) occurs at -21 mV, and the second (0.8A/F) occurs at -35 mV. The occurrence of the second late I_{Na} peak is due to a different mechanism than the first. The first peak is due to mutation-induced faster channel recovery from inactivation and then re-inactivation as the secondary depolarization, carried by Ca²⁺, results in more positive membrane potentials that favor inactivation. The second late I_{Na} peak is much smaller and occurs because of reactivated channels that are again recovering from inactivation. In this case, the repolarizing membrane is less favorable to inactivation and channels reopen before deactivating in response to further repolarization.

Here we show that this computational approach allowed us to determine subtle changes in channel gating that previously had not been investigated within the context of alteration in cellular repolarization. It must be noted, however, that modeling of complex biological processes is not without limitations. By definition, a model is a simplification of the actual biological process that allows for insight and understanding but may result in the exclusion of details necessary for absolute understanding of biological complexity and mechanism. Nonetheless, the combination of theoretical prediction and experimental verification has led to the identification of a novel mechanism through which altered Na⁺ channel activity can account for prolonged QT intervals in mutation carriers. Although the waveform of the cardiac action potential and the electrical properties that define its plateau phase are unique, this integrative approach is applicable to understanding the molecular basis of other congenital diseases, such as myotonia and epilepsy, in which subtle changes in Na⁺ channel gating may increase the contribution of channel reopenings to myotonic discharge (myotonias)^{25–28} or bursts of neural activity (epilepsy and seizure disorders).^{5,29}

Acknowledgments

This work was supported by grants 1R01-HL 56810-5 and 1P01-HL 67849-02 from the National Institutes of Health, Heart, Lung and Blood Institute (Dr Kass).

References

- Marban E. Cardiac channelopathies. *Nature*. 2002;415:213–218.
- Jentsch TJ. Neuronal KCNQ potassium channels: physiology and role in disease. *Nat Rev Neurosci*. 2000;1:21–30.
- Jentsch TJ, Schroeder BC, Kubisch C, et al. Pathophysiology of KCNQ channels: neonatal epilepsy and progressive deafness. *Epilepsia*. 2000; 41:1068–1069.
- Schwake M, Friedrich T, Jentsch TJ. An internalization signal in CIC-5, an endosomal Cl-channel mutated in Dent's disease. *J Biol Chem*. 2001; 276:12049–12054.
- Lossin C, Wang DW, Rhodes TH, et al. Molecular basis of an inherited epilepsy. *Neuron*. 2002;34:877–884.
- Jurkat-Rott K, Lehmann-Horn F. Human muscle voltage-gated ion channels and hereditary disease. *Curr Opin Pharmacol*. 2001;1:280–287.
- Kullmann DM. The neuronal channelopathies. *Brain*. 2002;125: 1177–1195.
- Wang Q, Shen J, Splawski I, et al. *SCN5A* mutations associated with an inherited cardiac arrhythmia, long QT syndrome. *Cell*. 1995;80:805–811.
- Bennett PB, Yazawa K, Makita N, et al. Molecular mechanism for an inherited cardiac arrhythmia. *Nature (Lond)*. 1995;376:683–685.
- Clancy CE, Rudy Y. Linking a genetic defect to its cellular phenotype in a cardiac arrhythmia. *Nature (Lond)*. 1999;400:566–569.
- Nuyens D, Stengl M, Dugarmaa S, et al. Abrupt rate accelerations or premature beats cause life-threatening arrhythmias in mice with long-QT3 syndrome. *Nat Med*. 2001;7:1021–1027.
- An RH, Wang XL, Kerem B, et al. Novel LQT-3 mutation affects Na⁺ channel activity through interactions between alpha- and beta1-subunits. *Circ Res*. 1998;83:141–146.
- Rivolta I, Clancy CE, Tateyama M, et al. A novel *SCN5A* mutation associated with long QT-3: altered inactivation kinetics and channel dysfunction. *Physiol Genomics*. 2002;10:191–197.
- Abriel H, Cabo C, Wehrens XH, et al. Novel arrhythmogenic mechanism revealed by a long-QT syndrome mutation in the cardiac Na(+) channel. *Circ Res*. 2001;88:740–745.
- Clancy CE, Rudy Y. Na(+) channel mutation that causes both Brugada and long-QT syndrome phenotypes. a simulation study of mechanism. *Circulation*. 2002;105:1208–1213.
- Noble D. Modeling the heart: from genes to cells to the whole organ. *Science*. 2002;295:1678–1682.
- Noble D. The rise of computational biology. *Nat Rev Mol Cell Biol*. 2002;3:459–463.
- Noble D. Unraveling the genetics and mechanisms of cardiac arrhythmia. *Proc Natl Acad Sci U S A*. 2002;99:5755–5756.
- Chandra R, Starmer CF, Grant AO. Multiple effects of KPQ deletion mutation on gating of human cardiac Na⁺ channels expressed in mammalian cells. *Am J Physiol*. 1998;274:H1643–H1654.
- Wang DW, Yazawa K, George ALJ, et al. Characterization of human cardiac Na⁺ channel mutations in the congenital long QT syndrome. *Proc Natl Acad Sci U S A*. 1996;93:13200–13205.
- Luo CH, Rudy Y. A dynamic model of the cardiac ventricular action potential: I: simulations of ionic currents and concentration changes. *Circ Res*. 1994;74:1071–1096.
- Patton C. WEBMAXCLITE v1.15. Available at: <http://www.stanford.edu/~cpatton/webmaxclite115.htm>. Accessed March 27, 2003.
- Cardiac Bioelectricity Research and Training Center. Research. Available at: <http://www.cwru.edu/med/CBRTC/Research.html>. Accessed March 27, 2003.
- Schwartz PJ, Priori SG, Spazzolini C, et al. Genotype-phenotype correlation in the long-QT syndrome: gene-specific triggers for life-threatening arrhythmias. *Circulation*. 2001;103:89–95.
- Wang DW, VanDeCarr D, Ruben PC, et al. Functional consequences of a domain I/S6 segment sodium channel mutation associated with painful congenital myotonia. *FEBS Lett*. 1999;448:231–234.
- Jurkat-Rott K, Mitrovic N, Hang C, et al. Voltage-sensor sodium channel mutations cause hypokalemic periodic paralysis type 2 by enhanced inactivation and reduced current. *Proc Natl Acad Sci U S A*. 2000;97: 9549–9554.
- Desaphy JF, De Luca A, Tortorella P, et al. Gating of myotonic Na channel mutants defines the response to mexiletine and a potent derivative. *Neurology*. 2001;57:1849–1857.
- Green DS, George AL Jr, Cannon SC. Human sodium channel gating defects caused by missense mutations in S6 segments associated with myotonia: S804F and V1293I. *J Physiol*. 1998;510:685–694.
- Wang DW, Viswanathan PC, Balsler JR, et al. Clinical, genetic, and biophysical characterization of *SCN5A* mutations associated with atrioventricular conduction block. *Circulation*. 2002;105:341–346.